Solid State Science and Technology, Vol. 15, No 2 (2007) 34-43
ISSN 0128-7389

PHOTOTHERMAL STUDY OF ZnO CERAMIC DOPED WITH TiO_2

A. Zakaria, Z. Rizwan, S. A. Halim, W. M. M. Yunus, M. Hashim

Department of Physics, Faculty of Science, Universiti Putra Malaysia, 43400 UPM Serdang, Selangor, Malaysia

ABSTRACT

Photopyroelectric spectroscopy (PPES) is a useful tool for examining non-radiative de-excitation in semiconductor materials. The ceramic (ZnO-x, x = 0.4-2.7 mol % of TiO2) was sintered at an isothermal temperature of 1270 °C for 1 and 2 hours to investigate its optical properties. The PPES is used to study the energy band gap of this ZnO system with reference to TiO_2 doping level. The energy band-gap obtained from photopyroelectric spectrum is about constant at 2.82 eV for the samples sintered for 2 hour at all TiO_2 doping levels except at 0.4 mol.% which is 2.78 eV. The energy band gap decreases with the decrease of sintering time from 2 to 1 hour at all doping levels and is about constant at 2.79 eV for the sintering time of 1 hour except that at 0.6 mol.% level which is 2.84 eV. The steepness factors σ_A and σ_B which characterize the slop of exponential optical absorption are discussed with reference to the TiO_2 doping level. The X-ray diffractrometry shows that the crystal structure of ZnO doped with different TiO_2 mol% remains to be of hexagonal type. Microstructure and compositional analysis of the selected areas are analyzed using SEM and EDAX. The maximum relative density 95.16 % is obtained for the ceramic. The grain size is about constant at 26.8 – 311.6 μm up to 1 mol % of TiO_2 and then decreases with the increase of TiO_2 mol % indicating the excess TiO_2 suppresses the grain growth.

INTRODUCTION

Zinc Oxide (ZnO) a white polycrystalline solid material is a n-type semiconductor material with a large energy band-gap, 3.2 eV [1]. It crystallizes into a wurtzite structure, and is a complete hexagonal closed-packed (hcp) lattice with oxygen atoms inserted into the zinc hcp-lattice. It is widely used in the manufacturing of paints, rubber products, cosmetics, pharmaceuticals, floor covering, plastics, textiles, ointments, inks, soap, batteries, and also in electrical components such as piezoelectric transducers, phosphors, gas sensors and varistors [2, 3].

The lattice constants of ZnO vary depending on how great is the unavoidable deviation from stochiometry towards an excess of the metal ($Zn_{1+x}O$). There are different opinions about the type of point defects that occur in the ZnO. The fact that the bonds in ZnO are 50 - 60% ionic [4] gives no indications to the type of defects. The measurements of the electron density [5] have shown that dominant defects are interstitial zinc ions and it was confirmed by Hagemark *et al*. [6] and Li *et al*. [7]. Other investigators, however, suggest that it is oxygen vacancies V_o that predominates and this hypothesis never been refuted. The measurement of the content of excess zinc in $Zn_{1+x}O$

Corresponding Author: azmizak@fsas.upm.edu.my

has indicated that the value of x ranges from 0 to 0.7 depending on the temperature and oxygen partial pressure [8].

Varistors are extensively used as protective devices to regulate transient voltage surges of unwanted magnitudes [9]. The exact role of many additives in the electronic structure of ZnO varistors is uncertain. ZnO based varistor is formed with other metal oxides of small amounts such as Bi_2O_3, Co_3O_4, Cr_2O_3, MnO, Sb_2O_3 etc. These additives are the main tools that are used to improve the non-linear response and the stability of ZnO varistor [10]. Varistor effect (highly nonohmic behavior in the *I-V* characteristics), can be explained via a mechanism involving the grain boundaries and the associated defect concentration gradients [11]. The distribution of vacancies and impurities as well as their behavior during annealing treatments appear as one of the factors that determine the electrical properties of ceramic ZnO. Much work has been done in *I-V* studies on ZnO based varistor by previous workers [10, 12]. It is necessary to get information on optical absorption of ceramic ZnO doped with different metal oxides for the investigation on electronic states of ceramic ZnO and doped impurities during sintering process and in this paper we discuss the photopyroelectric spectroscopy of the TiO_2 doped ceramics ZnO.

MATERIALS AND METHODS

ZnO (99.9% purity, Alfa Aesar) was doped with TiO_2 (99.9% purity) 0.4, 0.6, 1.0, 1.7, 2.5 mol%. The 24 hours ball milled powder of each mole percent was pre-sintered at temperatures 700 °C for 2 hours. Then each sample was ground and polyvinyl alcohol (1.4 wt%) was mixed as a binder. The dried powder was pressed under a force of 800 kg cm^{-1} to form a disk of 10 mm diameter with 1 mm thickness. Finally the pellets were sintered at 1270°C for 1 and 2 hour in air at heating and cooling rate of 6°C min^{-1}. Density of all the sintered samples was measured by geometrical method [13] using the average of 10 disks for each sample. The mirror like polished samples was thermally etched for the microstructure analysis by SEM, Fig. 2, and the average grain size was determined by the grain boundary-crossing method. The disks of each sample were ground to make a fine powder for the photopyroelectric (PPE) spectroscopy and XRD analysis. Cu K_α radiation with PANAalytical (Philips) X'Pert Pro PW1830 was used for X-ray diffraction, and the XRD data were analyzed by using X'Pert High Score software for the identification of the crystalline phases.

PPE spectroscopy a powerful technique from photothermal science is a non-radiative tool [14] to study optical properties of the materials. The method is based on photothermal effect where the pyroelectric (PE) film transducer is used to detect the temperature variation from the light-induced periodic heating in the sample. When there is absorption of incident light, the non-radiative de-excitation processes with in the solid will cause the sample temperature to fluctuate, through heat diffusion to the surrounding PE film. Due to this temperature change, a PE voltage is observed in the PE film. The measurement of PPE signal amplitude using the PPE spectrometer system to produce a PPE spectrum has been described elsewhere [15]. In the system, a light beam from 1 kW

Corresponding Author: azmizak@fsas.upm.edu.my

Solid State Science and Technology, Vol. 15, No 2 (2007) 34-43
ISSN 0128-7389

Xenon arc lamp (Oriel 6921) was mechanically chopped at 9 Hz for scanning wavelengths range of 300 to 800 nm.
Prior the PPE measurement, the fine powder sample was ground in deionised water and then a few drops of each mixture were dropped on the 1.5 cm^2 aluminium foil and dried in air to form a thin sample layer on the foil. The foil was placed in contact to polyvinylidene difluoride PE film sensor [16] using a very thin silver conductive grease, Fig. 1. The true sample spectrum was obtained by normalisation with respect to the carbon black PPE spectrum. In determining the energy band-gap (E_g), it was assumed that the fundamental absorption edge of doped ZnO is due to the direct allowed transition. The optical absorption coefficient β varies with the excitation light energy $h\upsilon$ [17] and is given by the expression, $(\beta h\upsilon)^2 = C\,(h\upsilon - E_g)$ near the band gap, where $h\upsilon$ is the photon energy, C is the constant independent of photon energy, and E_g is the direct allowed energy band-gap. The PPE signal intensity ρ is directly proportional to β, hence $(\rho h\upsilon)^2$ is related to $h\upsilon$ linearly. From the plot of $(\rho h\upsilon)^2$ versus $h\upsilon$, the value of E_g is obtained by extrapolating the linear fitted region that crosses photon energy axis.

RESULTS AND DISCUSSION

The XRD pattern in, Fig. 1, shows all the samples have two phases, i.e. ZnO grains and intergranular layers. The Intergranular layers are composed of TiO_2 (ref. code 01-089-4203) and appears as a very small peaks in the XRD pattern. A secondary phase spinel (Zn_2TiO_4, ref. code 01-073-0578) is very clear at higher TiO_2 doping level for the both sintering times. [18]

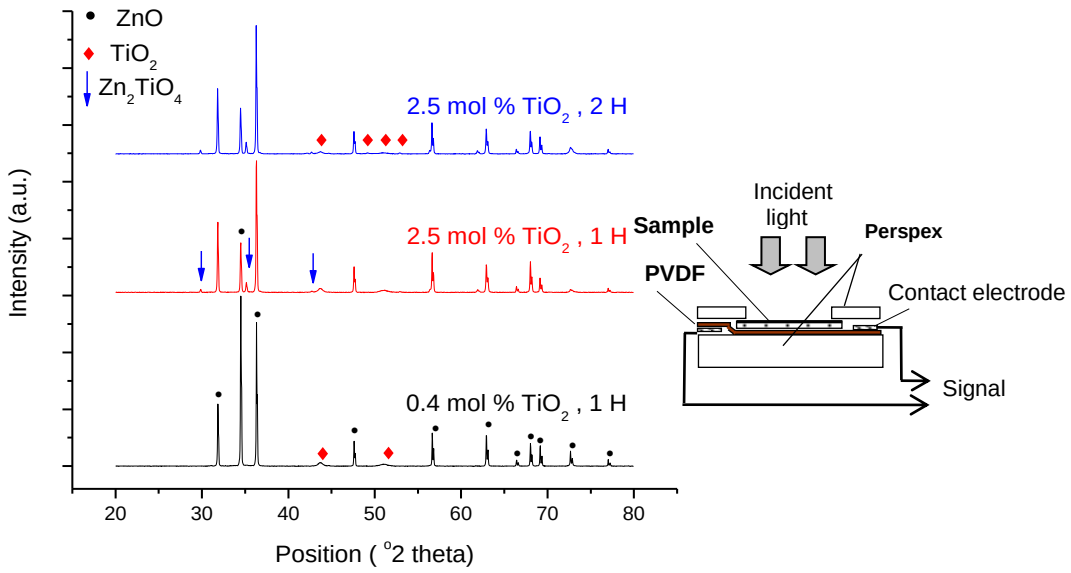

Fig. 1: XRD pattern for 1 and 2 hours sintering time (left); Schematic diagram of sample-PVDF holder (right).

Corresponding Author: azmizak@fsas.upm.edu.my

The density of the ceramics, Fig. 2, decreases from 94.12, 93.07% to 91.70, 91.60% of the theoretical density for 2 and 1 hours of sintering time, respectively up to the 1 mol% of TiO_2. Further increase of TiO_2 mol%, the density increases up to 95.16, 94.46% and again is decreased to 92.22, 91.86% for 2 and 1 hours of sintering time, respectively. This explains the ceramic density is not much affected with the increase of TiO_2 but for the combination at 1.7 mol%, the minimum pores are developed in the TiO_2 doped ceramic.

Grain size analysis, Fig. 2, shows that the grain size increases with the increase of sintering time from 1 to 2 hours. The grain size is about constant at 27, 30.5 µm up to 1 mol% of TiO_2 and then decreases to 13, 17.4 µm with the increase of the TiO_2 mol% for 1 and 2 hours of sintering time, respectively. The decrease in the grain size is due to the development of the sufficient amount of secondary phase Zn_2TiO_4 (spinel) which retards the grain growth mechanism [18]. SEM micrographs, Fig. 3, show that the grain boundaries and triple point junctions are well defined and are very clear. Optical micrographs show that the grains are elongated at lower TiO_2 mol% of for 1 hour sintering time but the corners become rounded slightly when the sintering time is increased from 1 to 2 hours. Some abnormal grain growth has been found in the ceramic structure.

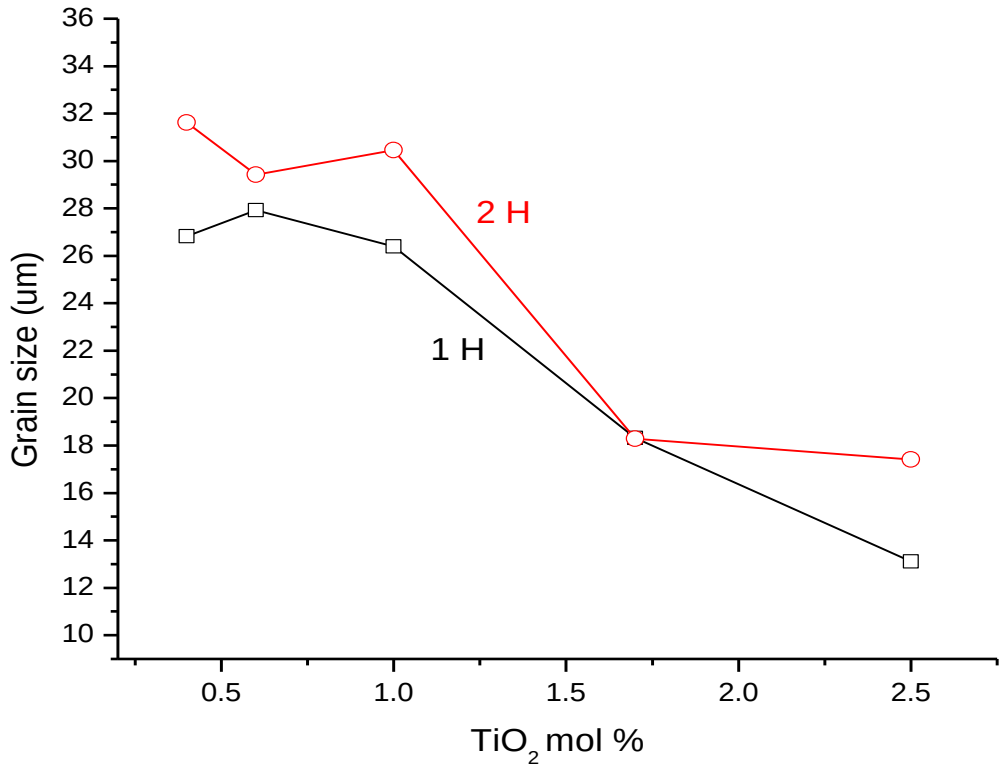

(a)

Corresponding Author: azmizak@fsas.upm.edu.my

Solid State Science and Technology, Vol. 15, No 2 (2007) 34-43
ISSN 0128-7389

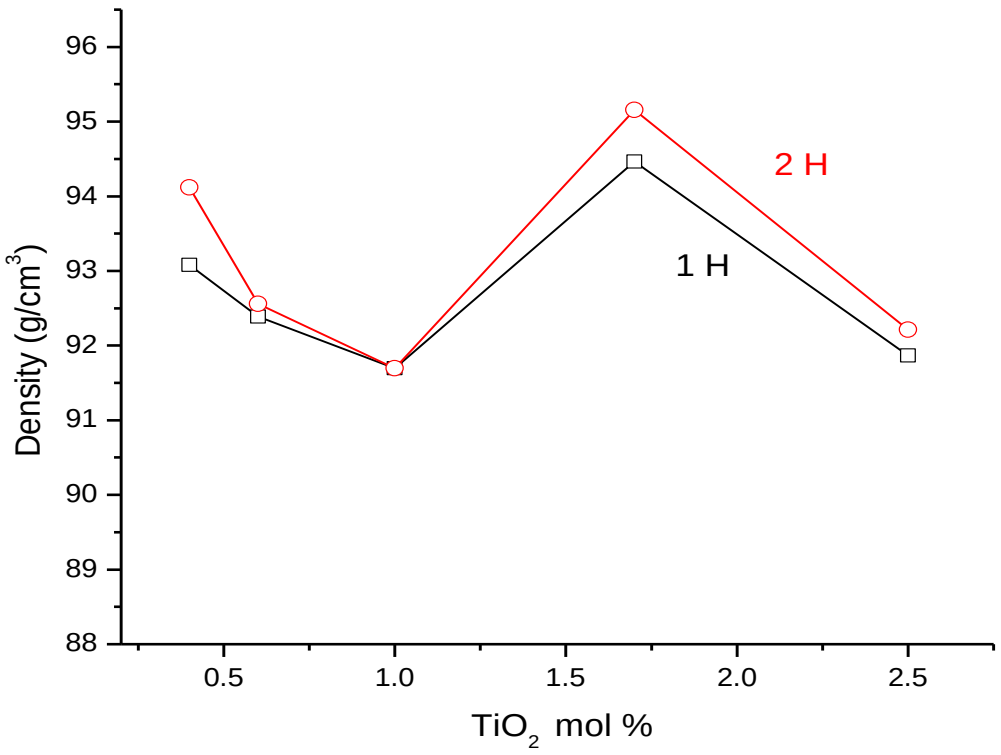

(b)

Fig 2: Density (a) and grain size (b) dependence on TiO_2 mol%, for 1 and 2 hours of sintering time.

At higher doping level of TiO_2 mol%, grains are more uniform but some small grains have been seen along with the big grains. EDAX analysis at the grain boundaries and at the surface of the grains show the absence of Ti^{2+} ions but some patches of titanium ions have been seen on the surface of the grains and near the nodal points. This explains that the Ti^{2+} ions, may be substituted in the ZnO lattice as the ionic radii of Titanium is smaller as compared to Zinc.

Energy band gap dependence on the TiO_2 mol% is shown in Fig. 4. E_g decreases to 2.79 eV at a doping level 0.4 mol%, and further increase of TiO_2, the value of E_g is about constant around 2.78 eV for 1 hour sintering time, except the value of E_g at 0.6 mol% which is 2.84 eV. The value of E_g is not affected with the increase of TiO_2 mol% but with the increase of the sintering time, the value of E_g affected in a very small quantity. The total variation in the value of E_g fluctuates with in the range of 0.08 eV with the change of doping level and sintering time. It is concluded that the reduction in E_g is due to the growth of interface states.

Corresponding Author: azmizak@fsas.upm.edu.my

Solid State Science and Technology, Vol. 15, No 2 (2007) 34-43
ISSN 0128-7389

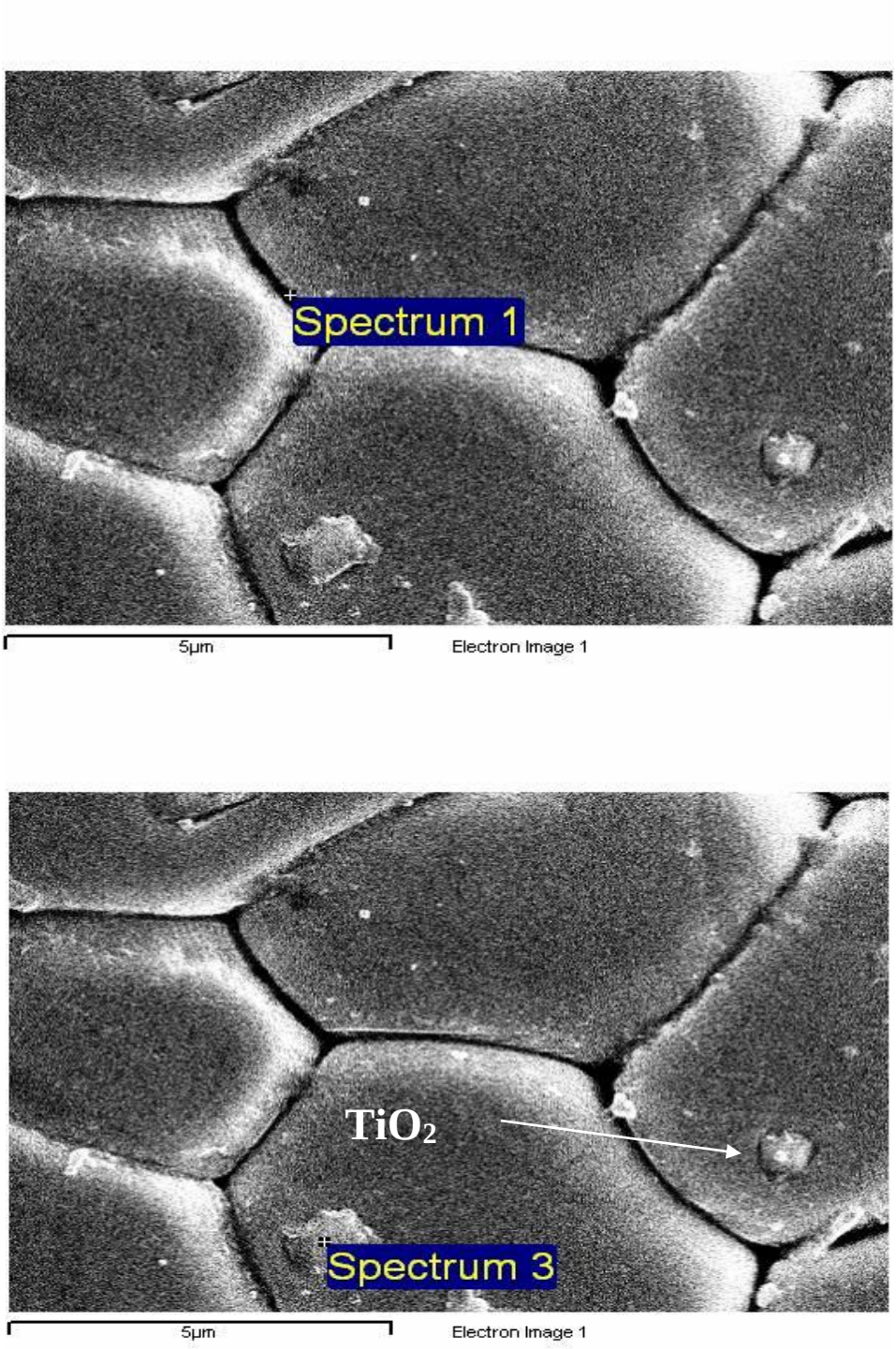

Fig. 3: SEM micrograph at 1.7 mol% TiO_2 for 1 hour sintering time.

Corresponding Author: azmizak@fsas.upm.edu.my

Solid State Science and Technology, Vol. 15, No 2 (2007) 34-43
ISSN 0128-7389

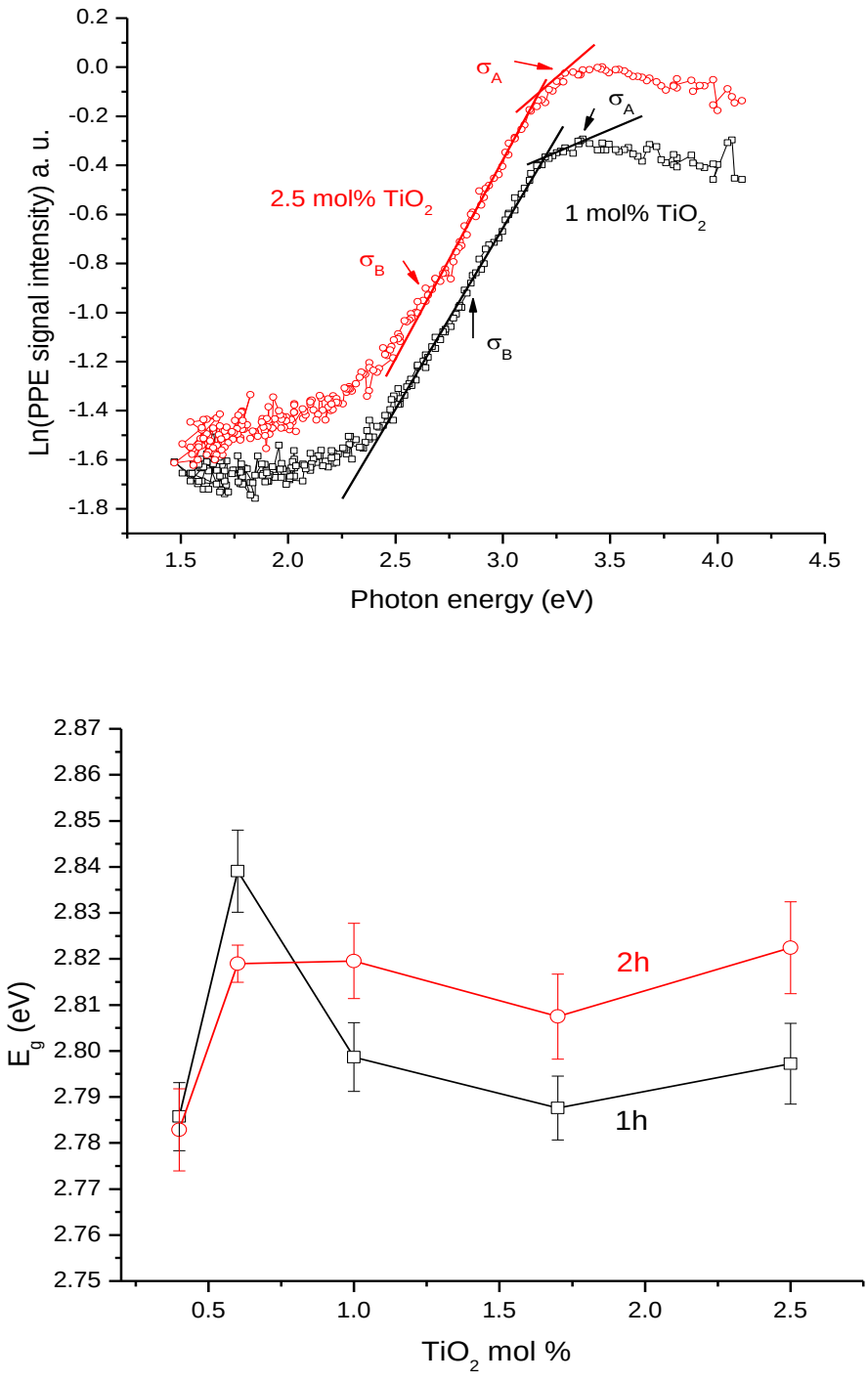

Fig 4: Energy band gap dependence on TiO_2 mol% (left), PPE signal intensity spectra for 1 hour sintering time (right).

Corresponding Author: azmizak@fsas.upm.edu.my

Solid State Science and Technology, Vol. 15, No 2 (2007) 34-43
ISSN 0128-7389

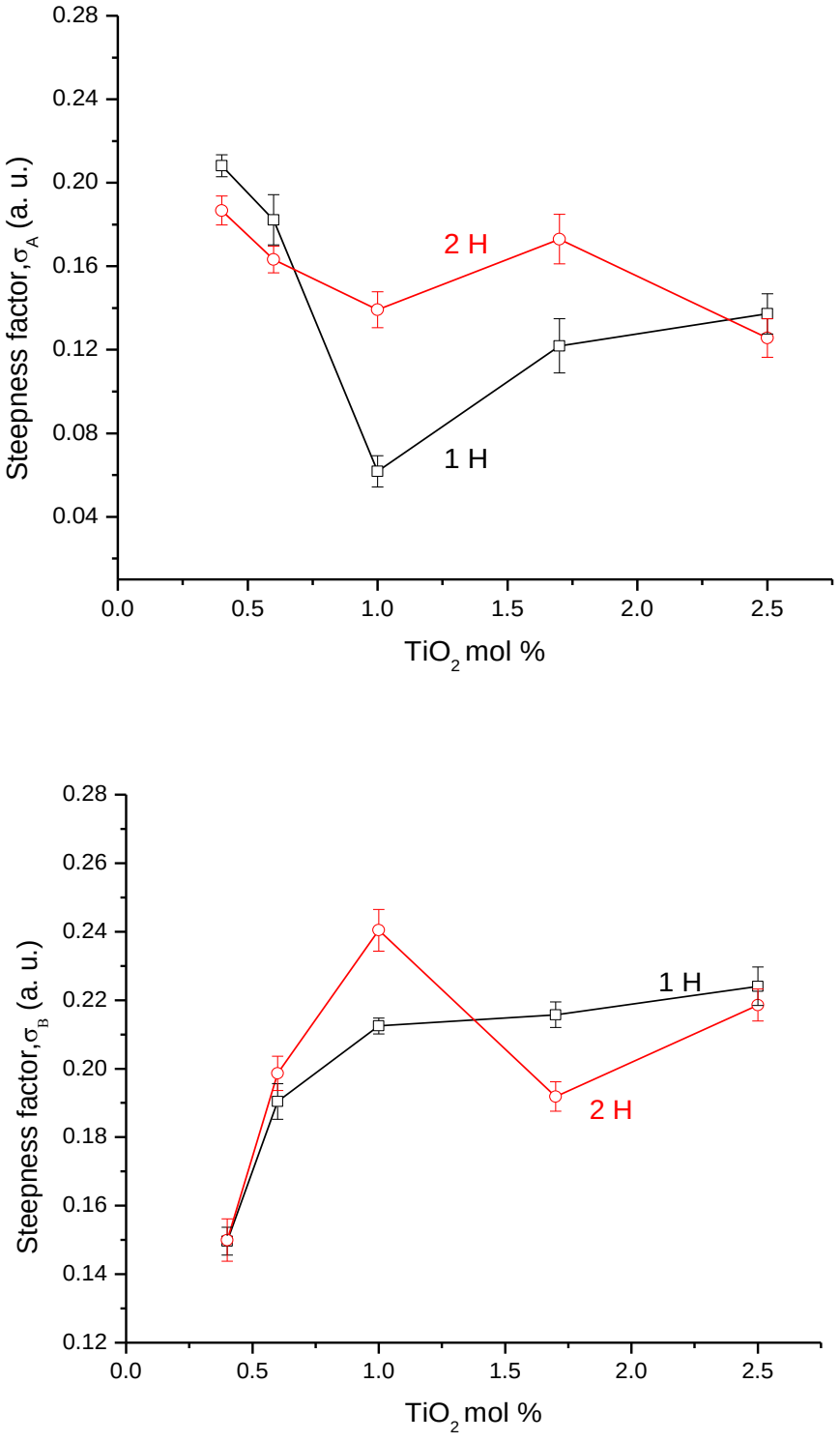

Fig. 5: Dependence of the steepness factor σ_A, (left), σ_B (right) on TiO_2 mol% for 1 and 2 hours sintering time.

Corresponding Author: azmizak@fsas.upm.edu.my

The steepness factor σ_A (in A-region), Fig. 5, which characterizes the slop of exponential optical absorption, sharply decreases from 0.20 to a minimum value 0.06 with the increase of TiO_2 mol% for 1 hour sintering time. For 2 hour sintering time, with the increase of doping mol%, a slow decrease of σ_A from 0.19 to minimum 0.13 value. Both minima occur at 1 mol% of TiO_2. This indicates the growth of interface states and can be incorporated with the decrease in E_g energy band gap.
The steepness factor σ_B (in B-region), which characterizes the slop of exponential optical absorption increases from 0.15 to 0.22 with the increase of TiO_2 mol% indicating the decrease in the defects for I hour sintering time. The value of σ_B increases from 0.15 to 0.21 with the increase of mol% indicating the further decrease in the defects for 2 hour sintering time.

CONCLUSION

The doping level of the TiO_2 and sintering times are correlated with the PPE spectroscopy. The energy band gap is decreased to 2.76 eV, may be due to the introduction of interface states but the all fluctuation remains in the limit of 0.08 eV. It was found that the energy band gap is not affected with the increase of TiO_2 mol % but it helps in the structuring ordering phenomena. EDAX analysis shows, that there is no segregation of TiO_2 at the grain boundaries and the substitution of Ti^{2+} ions in the ZnO lattice is expected. Extra phase Zn_2TiO_4 was found in the XRD patterns due to the TiO_2 which is responsible for the decrease of grain size especially after the 1 mol % of TiO_2

ACKNOWLEDGEMENTS

The authors would like to thank the Ministry of Science, Technology and Innovation of Malaysia for the financial support of this work under IRPA Grant No. 02-02-04-0132-EA001.

REFERENCES

[1] Gupta, T.K. (1990); Application of zinc oxide varistors, *J. Am. Ceram. Soc.*, **73(7)**, 1817-40.
[2] Lin, H.M., Tzeng, S.J., Hsiau, P.J. and Tsai, W.L. (1998); Electrode effects on gas sensing properties of nanocrystalline zinc oxide, *Nanostruct. Mater.*, **12**, 465-77.
[3] Look, D.C. (2001); Recent advances in ZnO materials and devices, Materials Science and Engineering, **B80**, 383-387.
[4] Neumann, G. (1981); Non-stoichiometry and defect structure, Kaldis E., (ed) *Currents Topics in Material Science*, Vol. **7** (Zinc Oxide), North Holland, Amsterdam, 153.
[5] Mohanty, G.P. and Azaroff, L.V. (1961); Electron density distribution in ZnO crystals, *J. Chem. Phys.*, **35(4)**, 1268.

Corresponding Author: azmizak@fsas.upm.edu.my

[6] Hagemark K.I. and Chacka, L.C. (1975); Electrical transport properties of Zn doped ZnO, *J. Solid State Chem.*, **15(3)**, 261.

[7] Li, P.W. and Hagemark, K.I. (1975); Low Temperature electrical properties of Zn doped ZnO, *J. Solid state Chem.*, **12(3/4)**, 371.

[8] Jae Shi Choi and Chul Hyun Yo (1976); Study of the Nonstoichiometric composition of zinc oxide, *J. Phys. Chem. Solids*, **37(12)**, 1149.

[9] David R. Clarke (1999); Varistor ceramics, *J. Am. Ceram. Soc.*, **8**, 485-501.

[10] Eda, K. (1989); Zinc Oxide Varistors, *IEEE Elect. Insul. Mag.*, **5**, 28-41.

[11] Einzinger, R. (1979); Grain junction properties of ZnO varistors, *Appl. Surf. Sci.*, **3**, 390-408.

[12] Choon-Woo Nahm (2003); Electrical properties and stability of praseodymium oxide based ZnO varistor ceramics doped with Er_2O_3, *J. Eu. Ceram. Soc.*, **23**, 1345-53.

[13] Wang, J.F., Wen-Bin Su, Hong-Cun Chen, Wen-Xin Wang, and Guo-Zhong Zang (2005); (Pr, Co, Nb)-doped SnO_2 Varistor Ceramics, *J. Am. Ceram. Soc.*, **88(2)**, 331-34.

[14] Minamide, A., Shimaguchi, M. and Tokunaga, T. (1998); Study on Photopyroelectric Signal of Optically Opaque Material Measured by PVD Film Sensor, *Jpn. J. Appl Phys.*, **37**, 3144-47.

[15] Mandelis, A. (1984); Frequency-domain photopyroelectric spectroscopy of condensed phases (PPES): A new, simple and powerful spectroscopic technique, *Chem. Phys. Lett.* **108**, 388-92.

[16] Tam, A.C. and Coufal, H. (1983); Photoacoustic generation and detection of 10-ns acoustic pulses in solids, *Appl. Phys. Lett.*, **42**, 33-35.

[17] Toyoda, T., Nakanishi, H., Endo, S. and Irie, T. (1985); Fundamental absorption edge in semiconductor $CdInGaS_4$ at high temperatures, *J. Phys. D Appl. Phys.*, **18**, 747-51.

[18] Bernik, S., Danue, N. and Recnic, A. (2004); Inversion boundary induced grain growth in TiO_2 or Sb_2O_3 doped ZnO based varistor ceramics, *J. Eu. Ceram. Soc.*, **24**, 3703-8.

Corresponding Author: azmizak@fsas.upm.edu.my